Orientational order at finite temperature on curved surfaces

J. Stat. Mech. (2016) 033208

(http://iopscience.iop.org/1742-5468/2016/3/033208)

Journal of Statistical Mechanics: Theory and Experiment
An IOP and SISSA journal

PAPER: Classical statistical mechanics, equilibrium and non-equilibrium

Orientational order at finite temperature on curved surfaces

Carolina Brito[1], Vincenzo Vitelli[2] and Olivier Dauchot[3]

[1] Instituto de Física, Universidade Federal do Rio Grande, do Sul CP 15051, 91501-970 Porto Alegre RS, Brazil
[2] Institute Lorentz for Theoretical Physics, Leiden University, NL 233 CA, Leiden, The Netherlands
[3] EC2M, UMR Gulliver 7083 CNRS, ESPCI ParisTech, PSL Research University, 10 rue Vauquelin, 75005 Paris, France
E-mail: carolina.brito@ufrgs.br

Received 11 December 2015
Accepted for publication 17 February 2016
Published 18 March 2016

Online at stacks.iop.org/JSTAT/2016/033208
doi:10.1088/1742-5468/2016/03/033208

Abstract. We study the effect of thermal fluctuations in the XY model on surfaces with unequal principal curvatures. Unlike Gaussian curvature that typically frustrates orientational order, the extrinsic curvature of the surface can act as a local field that promotes long-range order at low temperature. We find numerically that the transition from the high temperature isotropic phase to the true long-range ordered phase is characterized by critical exponents consistent with those of the flat space Ising model in two dimensions, up to finite size effects. Our results suggest a versatile strategy to achieve geometric control of liquid crystal order by suitable design of the underlying curvature of a substrate.

Keywords: classical Monte Carlo simulations, critical exponents and amplitudes, finite-size scaling, liquid crystals and bond-ordered phases

J. Stat. Mech. (2016) 033208

1742-5468/16/033208+10$33.00

Contents

Introduction

The interaction of geometry with orientational order and topological defects determines the spatial organization of many different systems [1], ranging from the bilayer membranes surrounding cells and intracellular organelles [2] to the thin-film patterns of block copolymers used to produce nanolithographic masks [3] or supramolecular assembly [4]. More broadly, understanding the spatial organization of soft systems under confinement is crucial for the success of new material design strategies based on self-assembly of thin layers or monolayers draped on curved substrates.

Spherical nematic shells are a paradigmatic illustration of the role of curvature and reduced dimensionality and they have been the subject of several experimental [5, 6] and theoretical investigations [7]. For thick shells, the nematic ground state is composed of two antipodally located pairs of three-dimensional defects called boojums. By contrast, for thin shells, the escape of the director in the third dimension is strongly penalized energetically: the shell behaves effectively as a two-dimensional system. This dimensionality reduction is marked by a qualitative change in the nematic ground state which displays four one-half disclinations rather than two pairs of boojums. The functionalization of such disclinations has been proposed as a route to endow spherical colloids with a four-fold valence [8].

One limitation associated with these quasi-two-dimensional systems is the lack of long-range order due to thermal fluctuations: on a flat substrate, two-dimensional systems with continuous symmetry and short-ranged interactions do not exhibit long-range order at finite temperature [9]. In principle, this limitation does not hold if the continuous symmetry is broken by coupling the order parameter to one of the principal axes of curvature of a deformed substrate. Seminal studies by Berreman have demonstrated that long-range orientational order is enhanced in a *three-dimensional* nematic sample bounded by a sinusoidally shaped wall [10]. However, in three dimensions, long-range orientational order is expected in the bulk even without confinement. The role of the curved wall is merely to enhance it in its proximity. In this article, we addess the distinct properties of monolayers or quasi-two-dimensional systems draped on a curved substrate and ask the following

J. Stat. Mech. (2016) 033208

question. Can the curvature of a substrate generate long-range orientational order where none is otherwise expected? We study in detail how curvature acts as an external ordering field that modifies the character of the Kosterlitz–Thouless transition in curved space.

The underlying curvature of a substrate can have an additional and opposite effect. If the surface possesses Gaussian (or intrinsic) curvature, geometric frustration will prevent the local orientational order dictated by physical interactions from propagating throughout the two-dimensional space [1]. Theoretical studies of thin liquid crystal layers or monolayers on curved surfaces have primarily focused on determining the ground state texture that emerges from this competition between orientational order and Gaussian curvature [2, 11–15]. However, in experimental systems, the embedding of the substrate in three dimensions is important—the order parameter (e.g. the nematic director or spin orientation) couples to the two directions of curvature independently [16–20]. For instance, studies of columnar or smectic phases on a curved substrate have revealed that the extrinsic curvature can act as an effective field that locally orients the direction of the layers in the ground state [16, 17]. However, much less is known about the interplay between these ordering fields arising from the extrinsic geometry and thermal fluctuations.

In what follows, we investigate the finite-temperature properties of an isotropic model of in-plane bond orientational order on substrates with unequal principal curvatures (eg. not simply spherical). We show within continuum elastic theory that orientational order in these curved spaces can be described as a *planar* XY model coupled to a position dependent external field. This ordering field competes against thermal fluctuations by promoting alignment of the order parameter along the local direction of smallest principal curvature. As a result, true long-range orientational order can take place at low temperature in quasi-two-dimensional systems draped on such curved substrates. On a generic surface (eg. one shaped as the bottom of an egg carton) the direction and strength of this ordering field will be spatially inhomogeneous smoothing out the phase transition into a crossover. In order to study how the Kosterlitz–Thouless transition is modified in a *homogeneous* sytem with curvature we conducted Monte Carlo simulations of the curved XY model on a model surface composed of cylindrical sectors alternately pointing upward and downward figure 1. In this test geometry, we find agreement with the results of our theoretical analysis that applies also to more complex substrates. Finite size scaling demonstrates that the critical exponents characterizing the transition from the high temperature isotropic phase to the low temperature ordered phase are consistent, up to numerical accuracy, to those of the planar Ising model.

Continuum elastic theory

Consider the Hamiltonian

$$H_{XY} = -J\sum_{\langle ij\rangle} \vec{s}_i \cdot \vec{s}_j \tag{1}$$

doi:10.1088/1742-5468/2016/03/033208

J. Stat. Mech. (2016) 033208

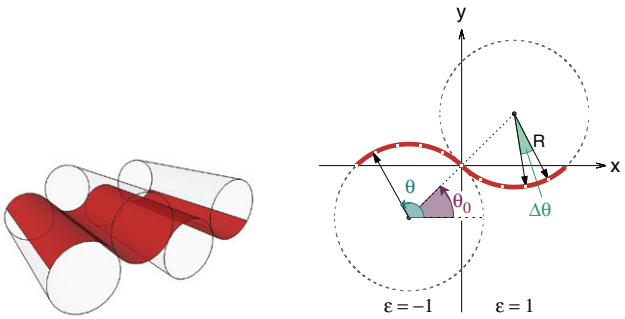

Figure 1. Left: The XY model is studied on a curved surface (red) composed of cylindrical sectors alternately pointing upward and downward. This surface has zero Gaussian, $\kappa = 0$ and constant mean curvature M, set by the cylinder radius R. **Right:** Cross-section of a unit cell. The cylinders are parallel to the z-direction and tangent at the origin. The red path is the surface where the spins centers—represented by the white dots—live.

of the classical XY model that describes unit length spins located on the node of a two-dimensional lattice with nearest neighbor interactions of strength $J > 0$. This simple model of orientational order exhibits the celebrated Kosterlitz–Thouless transition which is triggered by the unbinding of vortices and anti-vortices [21, 22] above the critical temperature $T_{\boldsymbol{KT}}$. In the low temperature phase $T < T_{\boldsymbol{KT}}$, the vortices are bound, there is only quasi-long-range order, and the correlation function of the spins decays algebraically with distance. If the spins are linearly coupled to an external field $B_{\mathbf{ext}}$, long-range order is restored: the transverse spin correlation function decays exponentially at large distance $C_T \sim \mathrm{e}^{-r/\xi_T}$, with $\xi_T = (J/B_{\mathbf{ext}})^{0.5}$ [23].

In the case of a curved substrate, the in-plane vector order parameter $\mathbf{s}(\mathrm{x}) = \cos\theta(x)\mathbf{e_1} + \sin\theta(x)\mathbf{e_2}$ where $\mathbf{e_1}$ and $\mathbf{e_2}$ are two orthonormal basis vectors tangent to the substrate and $\theta(x)$ is the local bond angle. Generalization to the case of n-atic order invariant under $\frac{2\pi}{n}$ rotation of the local bond angle is straightforward (e.g. $n = 2$ and $n = 6$ describe nematic and hexatic order respectively). A general continuum elastic energy for n-atic order on a curved substrate reads

$$H_\theta = \frac{K}{2}\int \mathrm{d}^2x\sqrt{g}\,g^{ij}(\partial_i\theta - A_i)(\partial_j\theta - A_j) \tag{2}$$

where K is an elastic constant proportional to n^2 and the microscopic exchange interaction [13]. In equation (2), g_{ij} denotes the metric tensor, g is its determinant and $A_i = \mathbf{e_1}\partial_\mathbf{i}\mathbf{e_2}$ is the spin connection that ensure parallel transport when covariant derivatives of the order parameter are taken. The energy H_θ generalizes the familiar continuum elastic energy of the planar XY model once the substitution $\nabla\theta \to \partial_i\theta - A_i$ is made. It suppresses gradients in the angle θ that measure the local orientation that the tangent vector makes with respect to its neighbours. At the same time, it captures the geometric frustration induced by the Gaussian curvature of the substrate embedded via the geometric gauge field A_i. In writing equation (2), anisotropic contributions to H_θ that occur in the case $n = 1$ (classical spins) and $n = 2$ (nematic liquid crystals) have been neglected. Note also that equation (2) needs to be supplemented with a Landau energy functional to account for variations in the *amplitude* of the order parameter.

J. Stat. Mech. (2016) 033208

Recent studies have revealed that the extrinsic curvature of the substrate can play an important role, neglected by H_θ, in minimizing gradients of a vector field tangent to a curved surface [16–20]. Upon decomposing the normal curvature of the vector field along the two principal directions of curvature of the surface, an additional contribution to the elastic energy is obtained [16–18]:

$$H_\beta = \frac{K}{2}\int \mathrm{d}^2x\sqrt{g}\,[\kappa_1^2\cos^2\beta + \kappa_2^2\sin^2\beta] \tag{3}$$

where $\beta(x)$ represents the angle that the tangent vector forms at position x with respect to the local principal direction with smallest curvature $\kappa_1(x)$ while $\kappa_2(x)$ denotes the largest principal curvature at the same location.

Equation (3) captures a coupling between bond orientational order and extrinsic curvature whose origin can be intuitively grasped as follows. Consider a cylindrical surface of radius R with a nematic director (or spin) aligned (i) along its azimuthal direction with curvature $\kappa_2 = \frac{1}{R}$ or (ii) along its height which has vanishing curvature $\kappa_1 = 0$. In both cases, the spins (or molecules) share a common orientation that makes the free energy in equation (2) vanish. However, case (ii) is energetically favorable because in case (i) the molecules are still rotating with respect to each other giving rise to a bending energy proportional to $1/R^2$. On a generic surface the molecules will still align along the direction of minimal curvature $\kappa_1(x)$ as obtained from minimizing equation (3) with respect to $\beta(x)$. Any local angular deviations $\delta\beta(x)$ will result in an energy penalty δE given by

$$\delta E = \frac{K}{2}\int \mathrm{d}^2x\sqrt{g}(\kappa_2(x)^2 - \kappa_1(x)^2)\delta\beta(x)^2 \tag{4}$$

Additional sources of couplings to the extrinsic curvature, neglected in this study, are possible depending on the symmetries of the order parameter and the specific model under consideration. The continuum elastic theory in equations (3)–(4) applies to an arbitrary surface with spatially varying (and unequal) principal curvatures. We note that such a surface, e.g. one shaped as the bottom of an egg cartoon, will have both mean and Gaussian curvature. In this case, however, the ordering field has spatially inhomegeneous orientation and strength as evidence by equation (4). The spatial inhomogeneity tends to smooth phase transitions into crossovers.

In order to study the effect of curvature on the Kosterlitz–Thouless transition and determine critical exponents, we concentrate on a homogeneous surface with zero Gaussian curvature $\kappa = (\kappa_1 \times \kappa_2) = 0$ and constant mean curvature $M = \frac{1}{2}(\kappa_1 + \kappa_2) = \frac{1}{2R}$. In this case the elastic energy can be mapped, aside from metric factors, to a flat space XY Hamiltoninan H_B in the presence of an external field:

$$H_B = -J\sum_{\langle ij\rangle}\vec{s}_i\cdot\vec{s}_j + \sum_i B_i\sin^2(\beta_i) \tag{5}$$

where β_i denotes the angle that $\vec{s}_i$ forms with respect to the external field $B_i = Ja^2/R^2(\vec{x}_i)$ at position $\vec{x}_i$ and a is the lattice constant of the square grid used to discretize the model. A similar mapping holds also for nematic order provided that a coupling of the form $\sin^4(\beta_i)$ is chosen, see [16, 17]. Hence, using straightforward trigonometric identies,

the finite temperature properties of vector or nematic order on a curved substrate with non-vanishing mean curvature are mapped to p-clock models with $p = 2$ or $p = \{2, 4\}$ respectively. In both cases one expects to recover the same universality class as the Ising model [24, 25].

Monte Carlo simulations

To test this scenario explicitly, we perform Monte Carlo simulations of the XY model described by equation (1) on a curved surface of zero Gaussian curvature composed of cylindrical sectors alternately pointing upward and downward, figure 1. It is constructed from the periodical repetition of a unit cell made of two cylinders sectors, parallel to the z-direction. The two cylinders' axes are respectively going through the centers $\Omega^{\pm} = (\pm R\cos(\theta_0), \pm R\sin(\theta_0), 0)$, with R the cylinders radius, so that the two cylinders are tangent at the origin. The path colored in red in figure 1 is the cross-section of our surface of interest. In a given cell n, a point of the surface $\vec{X}$ is parametrized by its coordinates:

$$\begin{aligned} x &= x_{O_n} + \epsilon(R\cos(\theta_0) - R\cos(\theta)) \\ y &= \epsilon(R\sin(\theta_0) - R\sin(\theta)) \\ z &= z \end{aligned} \tag{6}$$

where $x_{O_n} = 4(n-1)R\cos(\theta_0)$ is the center of the nth cell, where $n = 1 \,..\, \mathcal{N}_c$. $\epsilon = 1, -1$ when the surface is convex, respectively concave, and $\theta \in [\theta_0, \pi - \theta_0]$ indicates the angular position of the spin. A spin $\vec{s}_i$ has coordinates (s_i^{θ}, s_i^z) in the tangent frame defined by the unit vectors $\hat{e}_\theta = (\epsilon\sin(\theta), -\epsilon\cos(\theta))$ and $\hat{e}_z$. The principal curvatures are $\kappa_z = 0$ and $\kappa_\theta = \epsilon/R$. The Gaussian curvature $\kappa = \kappa_z \times \kappa_\theta = 0$, while the mean (or extrinsic) curvature is given by $M = (\kappa_z + \kappa_\theta)/2 = \epsilon/2R$. In each unit cell the number of spins is $N_\theta \times N_z$. Spins are regularly spaced on a square lattice, of mesh size $a = R\Delta\theta$, with $\Delta\theta = 2(\pi - 2\theta_0)/N_\theta$. Choosing a as the unit length scale, the curvature $M = a/2R = \Delta\theta/2$ is continuously tuned by changing R. θ_0 follows in order to keep N_θ constant. In the following $N_z = N_\theta$, so that the total number of spins per unit cell is always N_θ^2. Finite size effects are studied by increasing the number of unit cells in both x and z directions, leading to systems of linear size $L = \mathcal{N} \times N_\theta \times a$ and total number of spins $N = (\mathcal{N}N_\theta)^2$, where $\mathcal{N}$ is the linear number of unit cells. The above setting has the advantage of allowing for a separate analysis of the effects of curvature and system size.

After initializing the spin orientations according to a flat distribution, we use Monte Carlo simulations to minimize the energy of the system, following the single-spin-flip Metropolis algorithm [26]. We measure the averaged magnetization $\langle m \rangle = \left\langle \left\| \sum_i \vec{s}_i \right\| \right\rangle$, with the expression for m being:

$$m = \frac{\sqrt{\left(\sum_i s_i^z\right)^2 + \left(\sum_i s_i^\theta \sin(\theta_i)\right)^2 + \left(\sum_i s_i^\theta \cos(\theta_i)\right)^2}}{N},$$

its fluctuations and the transverse correlation $C_T(r)$:

$$C_T(r) = \langle s_i^\theta(\vec{r})\hat{\mathrm{e}}_\theta^i \cdot s_j^\theta(\vec{r}+\vec{r}')\hat{\mathrm{e}}_\theta^j\rangle,$$

where the last average $\langle\cdot\rangle$ runs over the spins that are distant by r. All measurements are made after the system reaches its asymptotic equilibrium state (usually 10^5 iterations per spin) and averaged over at least 100 initial conditions. We consider several system sizes with $N_\theta = 10, 20, 50, 100$ and $\mathcal{N} = 1, 2, 3, 4, 5$, that is a number of spins spanning from $N = (1\times 10)^2$ up to $N = (5\times 100)^2$.

Results

We first consider the low temperature regime, $T = 0.1 \ll T_{\mathrm{KT}}$. For finite but not too large system size, the XY model in a plane has a finite magnetization which decreases logarithmically with system size:

$$\langle m\rangle(T, L) = \langle m\rangle_0(T) - \frac{k_{\mathrm{B}}T}{4\pi J}\ln(L/a), \tag{7}$$

with $\langle m\rangle_0(T) \simeq 1$ when $T = 0.1 \ll T_{\mathrm{KT}}$. Figure 2(a) shows how the introduction of the extrinsic curvature qualitatively modifies this behavior. When $\Delta\theta > 0$, the magnetization decreases with system sizes following equation (7) until, for $L > L^*$, it saturates to a constant value $\langle m\rangle^\infty$, to which it tends to, when $L/a \to \infty$. It is easy to verify that the magnetization obeys a scaling relation $\langle m\rangle(\Delta\theta, L) = \tilde{m}(L/L^*(\Delta\theta))$, which is best illustrated in figure 2(b) introducing $Z = \langle m\rangle_0 - \langle m\rangle$ and $X = \ln(L/a)$, $Z^\infty = \langle m\rangle_0 - \langle m\rangle^\infty$ and $X^* = \ln(L^*/a)$. From this scaling, one extracts the dependence of L^*/a as a function of $\Delta\theta$ plotted in figure 2(c). For large enough $\Delta\theta$, $L^*/a \simeq \Delta\theta^{-1} = R/a$: the crossover length scale is simply the curvature radius. One also obtains the *finite* value of the magnetization in the thermodynamic limit, $\langle m\rangle^\infty = \langle m\rangle_0 - \ln(L^*(\Delta\theta)/a) \simeq \mathrm{Cst} + b\ln(\Delta\theta)$.

Finally, the transverse correlations $C_T(r)$ of the magnetization fluctuations decreases exponentially (figure 3(a)) and the transverse correlation length ξ_T scales like the inverse mean curvature

$$\xi_T \sim \Delta\theta^{-1} \sim R. \tag{8}$$

Recalling that for the planar XY model in the presence of an external field, one has $\xi_T \sim B_{\mathrm{ext}}^{-0.5}$ [23], the above results confirm the mapping anticipated theoretically between the extrinsic curvature and an external field with amplitude inversely proportional to R^2. We have thus shown that the XY model on a curved surface with zero Gaussian and finite mean curvatures exhibits a phase with true long-range magnetic order at low temperature.

We now analyze what kind of transition happens at fixed mean curvature when the temperature is increased. Figure 4 shows the average magnetization $\langle m\rangle$ and the magnetic susceptibility $\chi = \beta N_T(\langle m^2\rangle - \langle m\rangle^2)$ as a function of temperature T for different system sizes as well as their finite size rescaling across the transition. We observe the following phenomenology: (i) when temperature increases, the magnetization decreases and goes to zero above a given temperature, (ii) the magnetic susceptibility shows a sharp increase around the temperature where $\langle m\rangle$ goes to zero and (iii) when the system

J. Stat. Mech. (2016) 033208

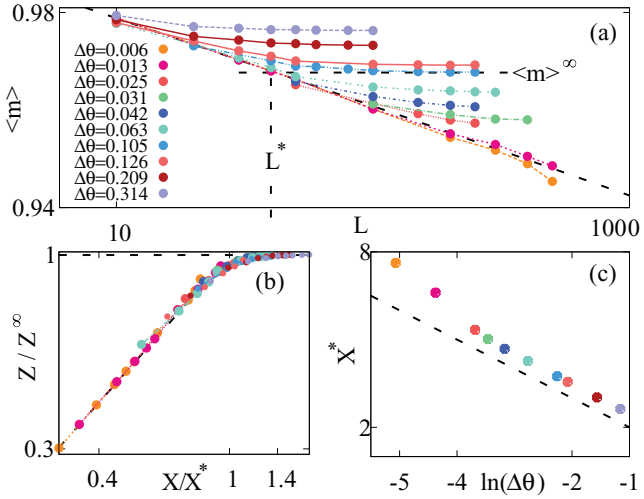

Figure 2. Magnetization at low T: (a) $\langle m \rangle$ as function of the system size L for various curvature $\Delta\theta$. Each point is an average over at least 100 initial conditions. The dashed line is the theoretical prediction for the zero curvature case (equation (7)) (b) Z/Z^{∞} versus X/X^{*}. The dashed line is $Z/Z^{\infty} = X/X^{*}$. (c) X^{*} versus $\ln(\Delta\theta)$. The dashed line indicates slope -1.

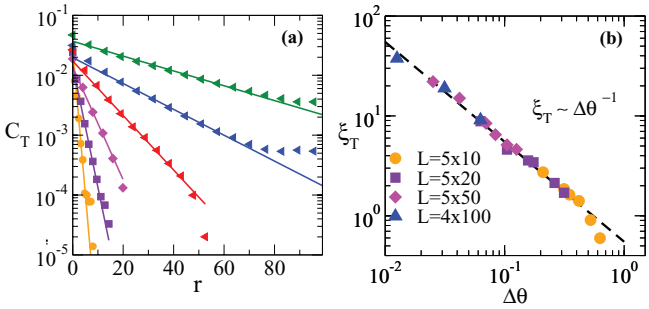

Figure 3. Transversal correlations: (a) $C_T(r)$ for different $\Delta\theta = [0.52, 0.26, 0.125, 0.063, 0.031, 0.013]$ and different system sizes (see legend in (b)). (b) Transversal correlation length ξ_T, extracted from exponential fits as shown in (a), as a function of $\Delta\theta$. The dashed line is a power-law fit with: $\xi_T \sim \Delta\theta^{-1}$.

sizes increase, χ becomes sharper. Since the curvature (akin to an external field) breaks the continuous symmetry of the spins, the system has now only two favored states. We then expect a phase transition similar to the Ising model [27]. To investigate this transition, we define the reduced temperature $t = (T - T_c)/T_c$ and investigate the following finite size scalings [28]:

$$\langle m \rangle = L^{-\beta/\nu} \tilde{m}(L^{-1/\nu} t), \tag{9}$$

$$\chi = L^{\gamma/\nu} \tilde{\chi}(L^{-1/\nu} t), \tag{10}$$

$$C = L^{\alpha/\nu} \tilde{C}(L^{-1/\nu} t), \tag{11}$$

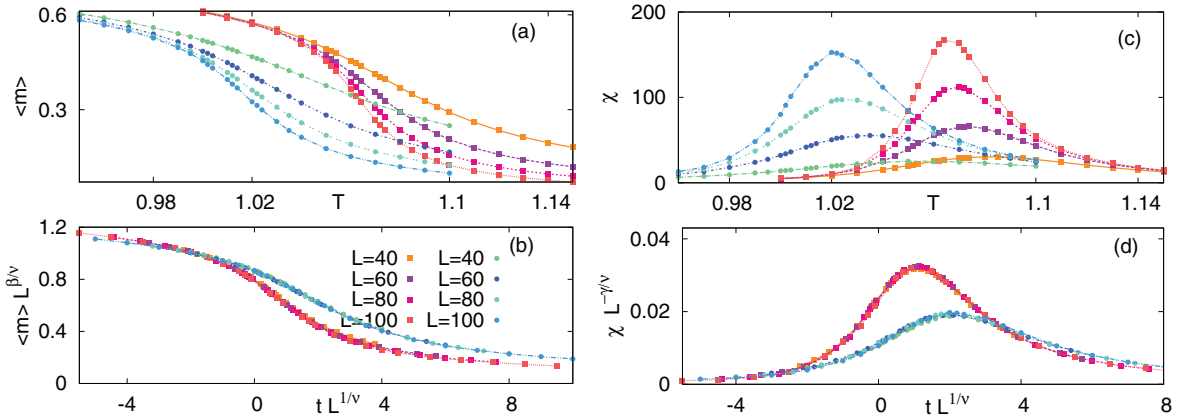

Figure 4. Magnetization $\langle m\rangle$ and magnetic susceptibility χ as a function of temperature. (a) $\langle m\rangle$ versus T (zoom on the transition). (b) Same data as (a) with $\langle m\rangle$ rescaled by $L^{\beta/\nu}$ and $t = (T - T_c)/T_c$ rescaled by $L^{1/\nu}$. (c) χ versus T (zoom on the transition). (d) Same data as (c) with χ rescaled by $L^{-\gamma/\nu}$ and $t = (T - T_c)/T_c$ rescaled by $L^{1/\nu}$. Squares are numerical data on the curved surface with fixed curvature $\Delta\theta_1 = \pi/10$ and circles correspond to a curvature of $\Delta\theta_2 = \pi/20$. The rescaling exponents are summarized in table 1.

where $C = \beta^2 N_T(\langle e^2\rangle - \langle e\rangle^2)$ is the specific heat with $\langle e\rangle$ the average energy per spin. We find $T_c = 1.055$, and $T_c = 1.000$ for the curvature $\Delta\theta_1 = \pi/10$, and $\Delta\theta_2 = \pi/20$ respectively. A study of the heat capacity, not shown here, reveals very small values for α, suggesting the existence of a logarithmic singularity with $\alpha = 0$, hence $\nu = 1$, as it is the case in the two-dimensional Ising model. In the following, we take those values for granted and perform a finite size scaling analysis on the magnetization and the susceptibility to obtain the exponents β and γ, which are summarized in table 1 together with the exponents of the Ising model in two dimensions.

Within numerical accuracy, we find consistent values for the critical exponent β for the two curved surface systems that are compatible with the two-dimensional Ising value for β. In contrast, the exponent γ depends slightly on the curvature: the smaller the curvature, the larger γ. Also the two-dimensional Ising model value for γ does not match our numerical data in the range of system sizes explored here. In practice L is never very much larger than the crossover size L^*, above which the system starts probing the curvature (see figure 2). We thus attribute our observations to the very strong finite size effects, associated with the essential singularity of the correlation length when approaching the Kosterlitz–Thouless transition from the high temperature phase [29]. Also, as the curvature is increased, the effect of the metric factors in equations (2) and (3), neglected in our mapping, becomes more important. This difference notwithstanding, our results suggest that in the thermodynamic limit, the XY model on the curved surface belongs to the two-dimensional Ising universality class.

In this work, we studied the interaction between the extrinsic geometry of a substrate and the orientational order of the system in the presence of thermal fluctuations. Using theoretical arguments and Monte Carlo simulations of a classical XY model confined to a surface with unequal principal curvatures, we showed that: (i) the extrinsic geometry acts as an external field and generates a true long order phase at low temperature and

Table 1. Estimated values of the critical exponents for two curvature $\Delta\theta_1 = \pi/10$, $\Delta\theta_2 = \pi/20$ and exact values for the Ising model in two dimensions.

Exponent	$\Delta\theta_1$	$\Delta\theta_2$	Ising
β	[0.11 0.17]	[0.11 0.17]	0.125
γ	[1.80 1.90]	[1.95 2.05]	1.75

(ii) when temperature increases, the system experiences a critical phase transition akin to the two-dimensional Ising model. Our work suggests an intuitive design criterion to experimentally realize surface morphologies that may achieve spatial control or modulation of in-plane orientational order in liquid crystal monolayers.

Acknowledgments

We thank the authors of [28] for very useful discussions about the FSS analysis and G Canova for sharing his data of the XY model on the plane with us. We also thank G Tarjus, R Kamien and A Souslov for helpful comments and discussions.

References

[1] Nelson D R 2002 *Defects and Geometry in Condensed Matter Physics* 1st edn (Cambridge: Cambridge University Press)
[2] Nelson D R, Piran T and Weinberg S 2004 *Statistical Mechanics of Membranes and Surfaces* (Singapore: World Scientific)
[3] Park M, Harrison C, Chaikin P M, Register R A and Adamson D H 1997 *Science* **276** 1401
[4] DeVries G A, Brunnbauer M, Hu Y, Jackson A M, Long B, Neltner B T, Uzun O, Wunsch B H and Stellacci F 2007 *Science* **315** 358
[5] Fernández-Nieves A, Vitelli V, Utada A S, Link D R, Márquez M, Nelson D R and Weitz D A 2007 *Phys. Rev. Lett.* **99** 157801
[6] Lopez-Leon T, Koning V, Devaiah K B S, Vitelli V and Fernandez-Nieves A 2011 *Nat. Phys.* **7** 391
[7] Vitelli V and Nelson D R 2006 *Phys. Rev.* E **74** 021711
[8] Nelson D R 2012 *Nano Lett.* **2** 1125
[9] Mermin N D and Wagner H 1966 *Phys. Rev. Lett.* **17** 1133
[10] Berreman D W 1972 *Phys. Rev. Lett.* **28** 1683
[11] Vitelli V and Turner A M 2004 *Phys. Rev. Lett.* **93** 215301
[12] Bowick M J and Giomi L 2009 *Adv. Phys.* **58** 449
[13] Park J-M and Lubensky T C 1996 *Phys. Rev.* E **53** 2648
[14] Shin H, Bowick M J and Xing X 2008 *Phys. Rev. Lett.* **101** 037802
[15] Bowick M, Nelson D R and Travesset A 2004 *Phys. Rev.* E **69** 041102
[16] Santangelo C D, Vitelli V, Kamien R D and Nelson D R 2007 *Phys. Rev. Lett.* **99** 017801
[17] Kamien R D, Nelson D R, Santangelo C D and Vitelli V 2009 *Phys. Rev.* E **80** 051703
[18] Selinger R L B, Konya A, Travesset A and Selinger J V 2011 *J. Phys. Chem.* B **115** 13989
[19] Vega D A, Gomez L R, Pezzutti A D, Pardo F, Chaikin P M and Register R A 2013 *Soft Matter* **9** 9385
[20] Napoli G and Vergori L 2012 *Phys. Rev. Lett.* **108** 207803
[21] Kosterlitz J M and Thouless D J 1973 *J. Phys. C: Solid State Phys.* **6** 1181
[22] Kosterlitz J M 1974 *J. Phys. C: Solid State Phys.* **7** 1046
[23] de Gennes P G and Prost J 1995 *Physics of Liquid Crystals* (Oxford: Oxford University Press)
[24] Lapilli C M, Pfeifer P and Wexler C 2006 *Phys. Rev. Lett.* **96** 140603
[25] José J V, Kadanoff L P, Kirkpatrick S and Nelson D R 1977 *Phys. Rev.* B **16** 1217
[26] Newman M E J and Barkema G T 1999 *Monte Carlo Methods in Statistical Physics* (Oxford: Oxford University Press)
[27] Yeomans J M 1992 *Statistical Mechanics of Phase Transitions* (Oxford: Oxford University Press)
[28] Canova G A, Levin Y and Arenzon J J 2014 *Phys. Rev.* E **89** 012126
[29] Janke W 1997 *Phys. Rev.* B **55** 3580